

1. Introduction

Data were acquired by the Advanced Microwave Precipitation Radiometer (AMPR) during the Cloud, Aerosol and Monsoon Processes Philippines Experiment (CAMP²Ex) field campaign in August-October of 2019.

These files include the Level 2B calibrated, corrected, and geo-referenced brightness temperature for the four AMPR-observed frequencies (10, 19, 37, 85 GHz). These data are archived in a self-describing, Climate and Forecasting (CF) 1.6-compliant Version 4 Network Common Data Format (netCDF4) format.

Python software has been developed for reading, plotting, and providing some additional analysis capabilities. This software is available from: <https://github.com/nasa/pyampr>. The AMPR instrument is explained in more detail here: <https://weather.msfc.nasa.gov/ampr/>.

These data have been determined to be viable for publishable scientific research, and also should be useful for generating quicklooks or understanding what happened during a flight. Note: AMPR is not expected to provide useful data during significant aircraft maneuvers.

AMPR is a significant project at MSFC. If you plan to use the final version of these data in a publication, please contact the principal investigator (PI), Timothy Lang (timothy.j.lang@nasa.gov), to discuss potential co-authorship.

2. Data Description

The primary data in these files are brightness temperatures at all AMPR frequencies and polarization channels (i.e., 10.7, 19.35, 37.1, and 85.5 GHz mixed-pol A/B channels, and for most flights deconvolved H and V polarizations).

Unvalidated geophysical retrievals of wind speed, water vapor, and cloud liquid water are included in files from 4 September 2019 onward. These retrievals are explained in Appendix F, and should only be considered when the aircraft is experiencing level, high-altitude flight.

In addition to the calibrated brightness temperatures, an objectively determined quality control (QC) metric is provided. The quality control metric is estimated based on the brightness temperature difference of a pixel within a 9x9 kernel of neighboring brightness temperatures. The QC metric is a discretized indicator of the difference within 5-Kelvin increments. Typical scene values fall in the QC 1 & 2 bins. However, very noisy scenes - generally indicative of instrument issues or potential scene contamination or excessive instrument noise - are isolated to values ≥ 4 . As with any objective measure based on thresholding, however, there is a gray area in the higher bins where some of the data is of high quality but physical phenomena are generating sharp, local features that are flagged as suspect. This, in and of itself, could be useful for those wanting to isolate features (e.g., the edges of a strong convective cell).

The radome used in CAMP²Ex had increased transmissivity loss near scan edges. While much of these data are still good, the end user is cautioned against blanketly accepting features seen near scan edges at face value. Therefore, as a precautionary measure, all data in the cross-track dimension pixels 0-9 and 40-49 have been flagged with QC = 8 (see example in Fig. 1).

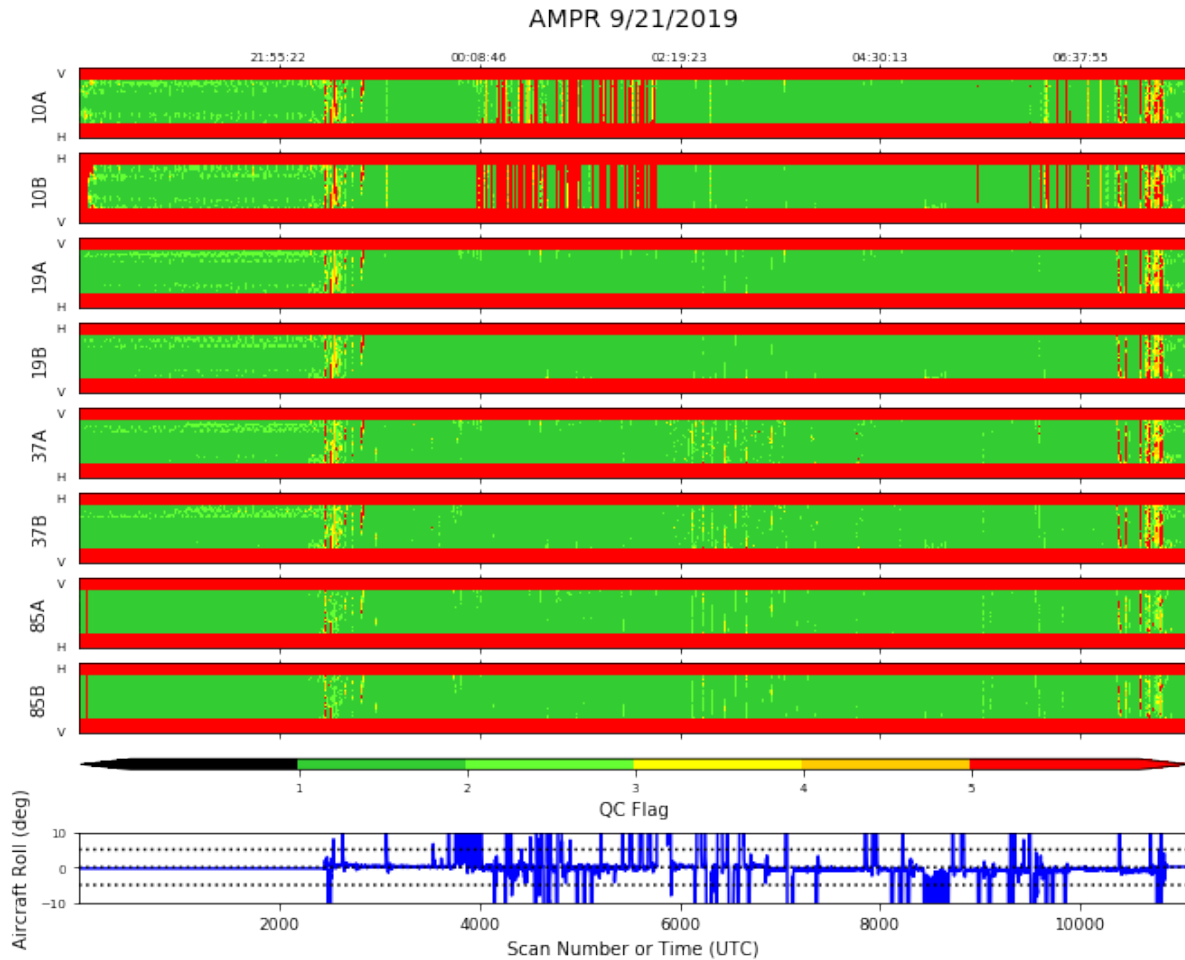


Figure 1. Strip chart of QC fields for AMPR channels during the 21 September 2019 flight, showing the scan edge flagging.

An incidence angle flag has also been included for quickly identifying pixels associated with large incidence angles typically encountered during aircraft roll maneuvers. During a roll, often the edge pixels began to see very large incidence angles or may even contain off-Earth sidelobe contamination. But, non-edge pixels may still be receiving observations from a typical/moderate (say -45° to 45°) incidence angle. Thus, we have opted for use of incidence angle flagging directly versus simply eliminating entire scans when the $|\text{roll angle}|$ is greater than a threshold.

Pixel field of view (FOV) water fractions are included. A 1-km gridded land/water fraction dataset - constructed from 250-m Moderate Resolution Imaging Spectroradiometer (MODIS) land/water mask (<https://lpdaac.usgs.gov/products/mod44wv006/>) - has been used, together

with the instrument FOV beamwidths to estimate the percent FOV that contains surface-water features. These data can be used to quickly identify (and eliminate if desired) those pixels originating from a mixed-surface (land and water) scene. The 250-m MODIS land/water mask includes water flagging for inland water bodies. However, no land-water mask is perfect, and it is possible that some smaller inland water bodies are missed. If so, then our FOV estimates will also be missing the water fraction contributions in such cases.

AMPR did not operate during CAMP²Ex flight #1 (20190824) and therefore no data from that flight are available.

Finally, AMPR was occasionally run in a pure nadir staring mode during overflights of certain clouds. These times are identified using the NadirFlag variable in the R0 dataset. AMPR geolocation during these times has been corrected, and these time periods should be considered as ScanAngle = 0°. Though this indicates effectively a 1D time series mode, the data are still structured using along-track and (faux) cross-track dimensions. The end user will need to unravel this 2D structure in order to develop a high-resolution time series. When developing the time series, note that AMPR spends 50 ms dwell time at each cross-track pixel. Note that, when plotting as a 2D structure (e.g., strip charts), nadir staring leads to data that are highly homogeneous in the (faux) cross-track direction.

3. Identifying Likely Good Data

As an example to quickly identify typical good data, a series of flagging based on the following conditions may be used:

QC incidence angle = 1
Pixel FOV < 0.1 or pixel FOV > 0.9 (i.e., mostly land or mostly water)
QC flag value <= 4

It is possible that sharp but valid contrasts near precipitation/clouds edges will be flagged by this. In addition, there may be good data near scan edges that is otherwise blanketly masked as QC = 8 for cautionary purposes (see above). Thus, recommended usage of these criteria is only as a guide and not an objective mask.

A level_flight_flag variable is in all files. This flag, which is derived from aircraft parameters (see Appendix B), tells whether to expect AMPR H/V deconvolution and geophysical retrievals (e.g., wind speed, water vapor, cloud liquid water) to be of the highest quality. This flag is set very conservatively, and it is possible that “non-level” flight segments still have valid deconvolution and retrievals.

Geophysical retrievals and polarization deconvolution data are not valid during nadir staring.

For test and science flights prior to 20190904, receiver gains and offsets were not optimized for AMPR channels 10B, 37A, and 85A. When these channels’ receivers equalized to the colder

temperatures experienced during high-altitude flight, radiometer counts and brightness temperatures became invalid. This effect has not been corrected, and thus flights prior to 9/4 have not had any radome correction, polarization deconvolution, or geophysical retrievals provided in the R0 dataset. These periods are also not well flagged by the automatic QC variable. Therefore, the end user is cautioned against using high-altitude flight data (> 3000 m MSL) from the 10B, 37A, and 85A channels prior to 9/4.

Appendix A. AMPR File Structure

Notable variables in AMPR data files are listed below.

(Note: Order in documentation does not necessarily match order in data files)

Dimensions

- AlongTrackDim = Variable, depends on flight length
- CrossTrackDim = 50
- BandDim = 4
- ChannelDim = 2 (pre-9/4) or 4 (9/4 and later)

AMPR-specific variables in all files

- float Frequency(BandDim)
- char Channel(ChannelDim) - A = Mixed-pol, left scan edge pure vertical, right scan edge pure horizontal; B = Opposite polarizations from A; H = Deconvolved horizontal polarization; V = Deconvolved vertical polarization.
- double Time(AlongTrackDim)
- double TB(ChannelDim, BandDim, AlongTrackDim, CrossTrackDim) - Brightness temperatures for all channels/bands.
- double ScanAngle(CrossTrackDim)
- double Lat(AlongTrackDim, CrossTrackDim)
- double Lon(AlongTrackDim, CrossTrackDim)
- double IncidenceAngle(AlongTrackDim, CrossTrackDim)
- double RelativeAzimuth(AlongTrackDim, CrossTrackDim)
- double LandFraction(BandDim, AlongTrackDim, CrossTrackDim)
- short QC(ChannelDim, BandDim, AlongTrackDim, CrossTrackDim)
- short IncidenceAngleQC(AlongTrackDim, CrossTrackDim)
- short NadirFlag (AlongTrackDim) - Flag indicating whether AMPR is staring nadir.

Additional AMPR-specific variables available in files 9/4 and later

- short precipitation_flag(AlongTrackDim, CrossTrackDim) - Flag indicating whether AMPR is likely observing precipitation. Geophysical retrievals are likely not valid in precipitation.
- short ice_scattering_flag(AlongTrackDim) - Flag indicating whether AMPR is likely observing ice scattering.
- double wind_speed_near_surface(AlongTrackDim, CrossTrackDim) - Radiometrically derived near-surface wind speed over the ocean.
- double atmosphere_water_vapor_content(AlongTrackDim, CrossTrackDim) - Radiometrically derived atmospheric water vapor content below the aircraft.
- double atmosphere_cloud_liquid_water_content(AlongTrackDim, CrossTrackDim) - Radiometrically derived cloud liquid water below the aircraft.

Aircraft-related data derived from corrected IWG1 feed

- short level_flight_flag (AlongTrackDim) - Flag indicating whether aircraft is experiencing conservatively defined level flight at altitude, indicating that AMPR polarization deconvolution and geophysical retrievals are of the highest quality
- double GPSAltitude(AlongTrackDim)
- double GPSLatitude(AlongTrackDim)
- double GPSLongitude(AlongTrackDim)
- double Pitch(AlongTrackDim)
- double Roll(AlongTrackDim)
- double Yaw(AlongTrackDim)
- double Head(AlongTrackDim)
- double WindDirection(AlongTrackDim) - This refers to wind direction at the aircraft's position
- double WindSpeed(AlongTrackDim) - This refers to wind speed at the aircraft's position
- double AirSpeed(AlongTrackDim)
- double GroundSpeed(AlongTrackDim)
- double Pressure(AlongTrackDim)
- double Temperature(AlongTrackDim)

Appendix B. Identification of High-Altitude, Level-Flight Segments

An important analysis performed on the AMPR data from CAMP²Ex was identification of high-altitude, level-flight segments. These flight segments limit issues with increased AMPR Earth-incidence angle as the aircraft roll/pitch angles increase, as well as data quality degradation that was observed in real-time during CAMP²Ex at lower altitudes, especially in the 10.7-GHz brightness temperature (T_b) values. The specific methods used to identify these segments from each flight are as follows.

1. Identify all AMPR scans where aircraft roll and pitch angles were 1° or less (2° or less for the 20190806, 20190919, and 20191003 science flights) and the GPS altitude of the P-3 aircraft was 3000 m or greater.
2. For these high-altitude, level-flight segments, ignore scans where the AMPR-derived land fraction was greater than 1% in the nadir pixel.
3. Visually examine the remaining scan numbers to identify relatively large groups of AMPR scans (i.e., approximately 20 consecutive scans or greater) that met the above criteria. If two subsequent groups of scans were separated by a small number of scans (i.e., approximately 20 scans or fewer) where these criteria were not met (e.g., for a quick adjustment of the aircraft's heading or altitude), allow the few scans associated with the brief aircraft adjustment to be included in the high-altitude, level-flight flags.
4. These high-altitude, level-flight flags were generated for all files from the 18 science flights during which AMPR operated, in addition to the 3 test flights.

Appendix C. Identification of AMPR's Nadir-Stare Mode

A new operating mode that was introduced for AMPR during CAMP²Ex was a nadir-stare mode, where AMPR would continuously sample data at 0° scan angle, rather than scanning across the swath ±45° from nadir. This was accomplished by noting that the time difference (Δt) between the start of consecutive AMPR scans under its typical cross-track scan strategy is greater than 3 seconds (e.g., up to 8 seconds when looking at the calibration targets), while the time between scan start times when in nadir mode is 2-3 seconds. In addition, several seconds were needed to switch into and out of nadir-stare mode, which was reflected by a large Δt between AMPR scans when this change was made. With these scan properties in mind, the following methods were used in the automated detection of nadir-stare mode for each flight.

1. Identify all instances where the Δt between consecutive AMPR scans was greater than 9 seconds. Check the Δt between 2 and 3 scans immediately before and immediately after each of these scans (that is, scans $i+2$ and $i+3$, as well as scans $i-2$ and $i-3$, with scan i being the large Δt observation). If the Δt over 2-3 scans after the "large Δt scan" was less than 3 seconds, flag the large Δt scan as the start of nadir-stare mode; if the Δt over 2-3 scans before the "large Δt scan" was less than 3 seconds, flag the large Δt scan as the end of nadir-stare mode.
2. Since it takes a relatively long time to switch into and out of nadir stare mode, the number of scans identified as the start of nadir mode and the end of nadir mode in Step #1 should be equivalent. If this is true, flag all scan numbers between each pair of nadir start times and nadir end times as nadir-stare mode. If the number of nadir-start times and nadir-end times do not match, print all "large Δt scan" numbers, plot Δt between AMPR scans around each of these scan numbers, and manually set the true start and end times of the nadir-stare mode.
3. The nadir-stare mode flags were generated for all files from the 18 science flights that AMPR operated during, in addition to the 3 test flights. AMPR geolocation was corrected during stare mode by setting scan angle to 0°. Note that the ScanAngle variable in each file is not valid during nadir stare. The true ScanAngle is 0°.

Appendix D. Identification of AMPR Pixels wherein Precipitation was Observed

The identification of precipitation within AMPR pixels was accomplished using threshold Tb values that were set for 37.1 and 85.5 GHz. The Tb thresholds used were 220 K for 37.1 GHz and 250 K for 85.5 GHz. Any pixels where the raw Tb values in either AMPR's mixed-pol A channel or B channel were greater than the threshold Tb values for both frequencies were flagged as precipitation. The specific methods used when generating this flag for all flights were:

1. Remove any pixels where the aircraft roll angle and/or pitch angle was 5° or greater. The use of a 5° threshold here compared to the 1-2° threshold used for the high-altitude, level-flight flag allowed for precipitation within regions of turbulence to be identified more easily.
2. Ignore pixels where the GPS altitude was less than 3000 m, and any pixels where the land fraction observed in the 37.1- or 85.5-GHz channels was 1% or greater.
3. Check the 37.1- and 85.5-GHz Tb values within all remaining pixels. If the observed Tb at 37.1 GHz was greater than 220 K and the observed Tb at 85.5 GHz was greater than 250 K, flag the pixel as likely containing precipitation.
4. Precipitation flags were generated for all science flights starting on 20190904.

Appendix E. Identification of AMPR Scans wherein Ice Scattering was Observed

During CAMP²Ex, the effects of ice scattering were observed by AMPR across a variety of scenes, including above relatively intense convection as well as within anvil regions extending downwind from intense convection. The presence of ice scattering within these anvil regions made it more difficult to identify ice based on Tb thresholds, since background Tb values in the lower-frequency channels beneath an anvil appeared very similar to clear air. In addition, the specific local minima Tb value associated with ice scattering varied among the science flights, with some 85.5-GHz values being very similar to that of a clear-ocean background during the same flight. Because of this, it was decided to examine local noisy decreases in raw 85.5-GHz radiometric counts (i.e., from Level 1 AMPR data files) to identify the presence of ice scattering. Since these thresholds also varied throughout any given flight, the method used to identify ice scattering was:

1. Visualize the Tb data from the entire flight at all four AMPR frequencies. Select a single AMPR scan number where the P-3 was flying over a clear-ocean scene with an aircraft roll angle around 0°.
2. Calculate the minimum and standard deviation of the raw 85.5-GHz radiometric counts in AMPR's A channel within this clear-air scan, as well as the minimum value in the raw 37.1-GHz radiometric counts in AMPR's A channel for this scan.
3. Calculate the minimum and standard deviation of Channel-A raw 85.5-GHz radiometric counts for all AMPR scans during the flight.
4. Remove any AMPR scans where the aircraft pitch and/or roll angles were 5° or greater, where the aircraft GPS altitude was less than 3000 m, and/or where the land fraction observed in the 37.1- and/or 85.5-GHz data for any pixel in the scan was 1% or greater.
5. For each scan that was retained after the check in Step #4 above, calculate the median value of the minimum 85.5-GHz radiometric count observed across the 50 AMPR scans that immediately preceded the selected scan number (i.e., calculate a "median minimum" count value).
6. Check the minimum 85.5-GHz radiometric count in the current scan. If this value was less than the "median minimum" 85.5-GHz count from the previous 50 scans minus the standard deviation in 85.5-GHz count calculated for the clear-air scan in Step #2 above, and if the median 37.1-GHz radiometric count in the current scan was greater than the minimum 37.1-GHz radiometric count observed in the clear-air scan in Step #2, flag the scan as containing ice-scattering effects.
7. The ice-scattering flags were generated were generated for all science flights starting on 20190904.

Appendix F. Brightness Temperature Correction and Initial Geophysical Retrievals

The correction of Tb values to compensate for the effects of the new radome that was flown with AMPR during CAMP²Ex was accomplished using a series of MATLAB codes that were originally written by Dr. Sayak Biswas and adapted for use with the CAMP²Ex data. The methods used were similar to those for AMPR's OLYMPEX/RADEX (Olympic Mountain Experiment/Radar Definition Experiment) data analysis as outlined in Amiot et al. (2020), but will be summarized here as well. A radiative transfer model (RTM) was used to simulate the Tb values that would be observed in every AMPR pixel during each CAMP²Ex science flight if the radome was not present. In addition, initial geophysical retrievals of cloud liquid water (CLW), atmospheric water vapor (WV), and 10-m wind speed over the ocean (WS) were performed using the multiple-linear regression equations that were developed for use with the OLYMPEX/RADEX data and presented in Amiot et al. (2020). The specific steps used in the Tb correction and geophysical retrievals were as follows.

1. Convert the raw Level 1 (L1) AMPR data from netCDF format to MATLAB file format.
2. Run the RTM to simulate the Tb values that would be observed by AMPR if the radome was not present. Files from the Global Data Assimilation System (GDAS) were downloaded for each CAMP²Ex flight, and the GDAS file from the time nearest the middle of each flight was used in the RTM for each case. These GDAS data were interpolated to AMPR's swath positions throughout the flight, and a land mask was applied to remove any pixels with land present. The RTM was run using the Rosenkranz models for cloud liquid water, oxygen, nitrogen, and water vapor (Amiot et al. 2020), along with an assumed ocean salinity of 33 ppt.
3. Perform a statistical retrieval on the RTM output using the multiple-linear regression equations and polynomial coefficients that were developed in Amiot et al. (2020). These equations for CLW, WV, and WS are:

$$\text{CLW (mm)} = a_0 + a_1 \cdot \ln(290 - T_{b19v}) + a_2 \cdot \ln(290 - T_{b19h}) + a_3 \cdot \ln(295 - T_{b85v}) + a_4 \cdot \ln(295 - T_{b85h}),$$

$$\text{WV (mm)} = a_0 + a_1 \cdot T_{b10v} + a_2 \cdot T_{b10h} + a_3 \cdot \ln(290 - T_{b19v}) + a_4 \cdot \ln(290 - T_{b19h}) + a_5 \cdot \ln(290 - T_{b37v}) + a_6 \cdot \ln(290 - T_{b37h}) + a_7 \cdot \text{SST},$$

$$\text{WS (m s}^{-1}\text{)} = a_0 + a_1 \cdot \ln(285 - T_{b10v}) + a_2 \cdot \ln(285 - T_{b10h}) + a_3 \cdot T_{b10v}^2 + a_4 \cdot T_{b10h}^2 + a_5 \cdot (T_{b10v} \cdot T_{b10h}) + a_6 \cdot T_{b19v} + a_7 \cdot T_{b19h} + a_8 \cdot T_{b19v}^2 + a_9 \cdot T_{b19h}^2 + a_{10} \cdot (T_{b19v} \cdot T_{b19h}), + a_{11} \cdot T_{b37v} + a_{12} \cdot T_{b37h} + a_{13} \cdot T_{b37v}^2 + a_{14} \cdot T_{b37h}^2 + a_{15} \cdot (T_{b37v} \cdot T_{b37h}) + a_{16} \cdot \text{SST},$$

where Tb is in K, the h and v subscripts indicate horizontally and vertically polarized deconvolved Tb values, respectively, the 10, 19, 37, and 85 subscripts indicate AMPR frequencies of 10.7, 19.35, 37.1, and 85.5 GHz, respectively, the "a" values are the regression coefficients, and SST is the median sea-surface temperature during the flight.

4. Write the L1 AMPR data and the statistical retrieval file from Step #3 above to a single netCDF file for each individual flight.
5. Convert the netCDF file in Step #4 above to MATLAB file format.
6. Run another RTM similar to the one in Step #2 above, but interpolate the temperature, relative humidity, height, and pressure information from the GDAS profiles to individual AMPR pixels, rather than applying a single interpolated value to the entire swath for each scan. The same RTM settings described in Step #2 were applied to this interpolated RTM as well.
7. Run the a MATLAB script to perform the Tb corrections and geophysical retrievals for each flight. Within this script, the raw L1 AMPR data, the interpolated RTM data, and the MATLAB file containing the L1 data and the statistical retrievals were imported. The A- and B-channel AMPR Tb data were converted to vertically and horizontally polarized Tb data for the scene using another MATLAB script. Excess Tb values were computed as the RTM-simulated Tb subtracted from the L1 Tb values within each AMPR pixel at each frequency and polarization. Slope and offset coefficients were computed for each AMPR frequency and polarization as:

$$\text{slope} = (T_{b,\text{hot}} - T_{b,\text{RTM}}) / (T_{b,\text{hot}} - T_{b,\text{obs}}),$$

$$\text{offset} = T_{b,\text{RTM}} - (\text{slope} \cdot T_{b,\text{obs}}),$$

where $T_{b,\text{hot}}$ is the Tb of the hot calibration target, $T_{b,\text{RTM}}$ is the Tb output from the RTM for the given pixel, and $T_{b,\text{obs}}$ is the observed Tb at the given frequency and polarization. Once these calculations were performed, the AMPR scan numbers corresponding to the high-altitude, level-flight segments from Appendix B were entered into the code for the Tb correction to be performed. Any scans where the aircraft roll angle was greater than 1-2° (depending on flight) were excluded from the analysis. In addition, all pixels where the observed L1 85.5-GHz Tb value was greater than the RTM 85.5-GHz Tb value by more than 8 K, which was identified from an empirical analysis as the minimum difference that would be applicable to all flights on or after 20190904, were flagged as precipitation and were excluded from the Tb correction. The slope and offset values from the “good scans” based on these exclusions were interpolated over time for every pixel in a given scan; the resulting interpolated slope and offset values were used as the slope and offset values for the Tb corrections via the relation

$$T_{b,\text{corr}} = (\text{slope} \cdot T_{b,\text{obs}}) + [(1 - \text{slope}) \cdot T_{b,\text{hot}}],$$

where $T_{b,\text{corr}}$ is the corrected Tb value for the given frequency, polarization, and AMPR pixel. The resulting corrected Tb values were then entered into the equations above for

CLW, WV, and WS to perform the geophysical retrievals. The corrected Tb values and the retrieved values of CLW, WV, and WS from the “good scans” within each flight were saved.

8. Corrected brightness temperatures and geophysical retrievals were generated for all science flights starting on 20190904. Geophysical retrievals have not yet been validated against independent data sources (e.g., dropsondes, etc.).

References

Amiot, C. G., S. K. Biswas, T. J. Lang, and D. I. Duncan, 2020: Dual-Polarization Deconvolution and Geophysical Retrievals from the Advanced Microwave Precipitation Radiometer during OLYMPEX/RADEX. Conditionally accepted in *J. Atmos. Ocean. Technol.* (contact Corey Amiot for copy: ca0019@uah.edu)